Pharmacokinetic Modeling of Warfarin I – Model-Based Analysis of Warfarin Enantiomers with a Target Mediated Drug Disposition Model Reveals *CYP2C9* Genotype-Dependent Drug-Drug Interactions of S-Warfarin[S]

Shen Cheng, Darcy R. Flora, Allan E. Rettie, ● Richard C. Brundage, and Timothy S. Tracy

Department of Experimental and Clinical Pharmacology, College of Pharmacy, University of Minnesota, Twin Cities, Minneapolis, Minnesota (S.C., D.R.F., R.C.B.); Tracy Consultants, Huntsville, Alabama (T.S.T.); and Department of Medicinal Chemistry, School of Pharmacy, University of Washington, Seattle, Washington (A.E.R.)

ABSTRACT

The objective of this study is to characterize the impact of the *CYP2C9* genotype on warfarin drug-drug interactions when warfarin is taken together with fluconazole, a cytochrome P450 (CYP) inhibitor, or rifampin, a CYP inducer with a nonlinear mixed effect modeling approach. A target-mediated drug disposition model with a urine compartment was necessary to characterize both S-warfarin and R-warfarin plasma and urine pharmacokinetic profiles sufficiently. Following the administration of fluconazole, our study found subjects with *CYP2C9* *2 or *3 alleles experience smaller changes in S-warfarin clearance compared with subjects without these alleles (69.5%, 64.8%, 59.7%, and 47.8% decrease in subjects with *CYP2C9* *1/*1, *1/*3, *2/*3, and *3/*3, respectively), whereas, following the administration of rifampin, subjects with *CYP2C9* *2/*3 or *CYP2C9* *3/*3 experience larger changes in S-warfarin CL compared with subjects with at least one copy of *CYP2C9* *1 or *1B (115%, 111%, 119%, 198%, and 193% increase in subjects with

CYP2C9 *1/*1, *1B/*1B, *1/*3, *2/*3, and *3/*3, respectively). The results suggest that different dose adjustments are potentially required for patients with different *CYP2C9* genotypes if warfarin is administered together with CYP inhibitors or inducers.

SIGNIFICANCE STATEMENT

The present study found that a target-mediated drug disposition model is needed to sufficiently characterize the clinical pharmacokinetic profiles of warfarin racemates under different co-treatments in subjects with various *CYP2C9* genotypes, following a single dose of warfarin administration. The study also found that S-warfarin, the pharmacologically more active ingredient in warfarin, exhibits *CYP2C9* genotype-dependent drug-drug interactions, which indicates the dose of warfarin may need to be adjusted differently in subjects with different *CYP2C9* genotypes in the presence of drug-drug interactions.

Introduction

4Although the use of new direct oral anticoagulants has increased recently, warfarin, a vitamin K antagonist, continues to be one of the

most extensively used oral anticoagulants worldwide (Barnes et al., 2015; Mak et al., 2019). However, despite being highly effective in preventing stroke and other thromboembolic events in patients with atrial fibrillation (Takahashi and Echizen, 2001; Hart et al., 2007), warfarin is notorious for its unpredictable pharmacokinetic (PK) and pharmacodynamic (PD) behaviors, narrow therapeutic index, and high between-subject variability (Ufer, 2005; Hamberg et al., 2007).

Warfarin is administered orally as a racemic mixture of R- and S-warfarin, in a 1:1 molar ratio. Following oral administration, warfarin enantiomers undergo rapid absorption and are almost completely bioavailable (Ufer, 2005). Although both enantiomers possess pharmacological activity, S-warfarin is much more potent than R-warfarin (Breckenridge et al., 1974; O'Reilly, 1974). Warfarin is eliminated primarily through hepatic metabolism with negligible urinary excretion (Lewis et al., 1974; Ufer, 2005). Various cytochrome P450 (CYP) enzymes are involved in the elimination of R- and S-warfarin to form multiple

---

ABBREVIATIONS: BL, baseline; BL$_P$, peripheral baseline; BQL, below the quantification limit; CI, confidence interval; CL, clearance; CL_Flu, fluconazole effect on clearance; CL$_R$, renal clearance; CL_Rif, rifampin effect on clearance; CYP, cytochrome P450; DDI, drug-drug interaction; DR, baseline level of drug-receptor complex compartment; EM, expectation-maximization; IIV, inter-individual variability; INR, international normalized ratio; IOV, inter-occasion variability; K$_a$, absorption rate constant; K$_{on}$, association rate constant; K$_{off}$, dissociation rate constant; LLOQ, lower limit of quantification; PD, pharmacodynamic; PK, pharmacokinetic; R, receptor; R$_{BL}$, baseline level of receptor compartment; RSE, relative standard error; RUV, residual unexplained variability; SIR, sampling importance resampling; TMDD, target-mediated drug disposition; TRT, treatment; VKORC1, vitamin K epoxide reductase complex subunit 1; VPC, visual predictive check.

monohydroxylated metabolites. S-warfarin is metabolized mainly through *CYP2C9*, whereas R-warfarin is metabolized through various CYP isoforms, such as *CYP1A2*, *CYP2C19,* and *CYP3A4* (Rettie et al., 1992; Ufer, 2005; Rettie and Tai, 2006).

CYP2C9 is susceptible to substantial genetic polymorphisms, with 15% of Caucasians carrying at least one functionally impaired allele of *CYP2C9* variants *2 (Arg144Cys) or *3 (Ile359Leu), which have been shown to be closely related to the reduced catalytic activity of CYP2C9 (Flora et al., 2017). Since *CYP2C9* is highly associated with the elimination of pharmacologically more active S-warfarin (Ufer, 2005), subjects with reduced *CYP2C9* metabolic status, attributable to *CYP2C9* *2 or *3 alleles, are subject to higher drug exposure and greater risk of dose-related toxicity. Indeed, studies have reported the *CYP2C9* genotype-dependent exposure of S-warfarin (Flora et al., 2017; Xue et al., 2017) as well as the association between *CYP2C9* genotype and the risk of warfarin-induced toxicity (Kawai et al., 2014).

Additionally, the *CYP2C9* regulatory polymorphism *1B (-3089G>A and -2663delTG) has been shown to be significantly associated with determining the maintenance dose of phenytoin because of its effect on phenytoin *CYP2C9* auto-induction (Chaudhry et al., 2010). Although *CYP2C9* *1B has been shown to have little impact on the dose of warfarin in various populations (Veenstra et al., 2005; Chaudhry et al., 2010), its impact on the clearance (CL) of warfarin following the administration of CYP inducers is unknown.

Considerable information has been curated regarding warfarin metabolism, pharmacogenetics, and drug-drug interactions (DDIs), and that information has been incorporated into several warfarin dosing algorithms (Gage et al., 2008; Finkelman et al., 2011; Kimmel et al., 2013; Asiimwe et al., 2021). Nonetheless, warfarin dosing remains challenging and a personalized medicine approach has not yet been realized. Additional complications continue to be uncovered, and a recent case report highlights the need for further investigations on the gene-DDIs of warfarin (Salem et al., 2021).

We previously reported the impact of *CYP2C9* genotypes on the PK or warfarin parent compounds and metabolites. (Flora et al., 2017). The present study is a comprehensive model-based analysis of the impact of *CYP2C9* genotype on warfarin DDIs when warfarin is administered together with CYP inhibitors and inducers. This manuscript is the first of a companion pair (Cheng et al., concurrently published) that extends the analysis using a rigorous nonlinear mixed effect model-based analysis that incorporates a target-mediated drug disposition (TMDD) model for warfarin. The scope of this paper is a model-based analysis of the impact of *CYP2C9* genotype on the DDIs of warfarin's (R) and (S) enantiomers following administration of the racemic mixture. Built upon the models developed for S- and R-warfarin in this study, the companion paper reports the model-based analysis of 10 warfarin metabolites, which contributes to the mechanistic understanding of *CYP2C9* genotype on the DDIs of warfarin enantiomers (Cheng et al., concurrently published).

Methods

Study Population. Study subjects were selected based on their *CYP2C9* genotypes from a pharmacogenetics registry (Flora et al., 2017). The *CYP2C9* genotyping was performed by the University of Minnesota Genomics Center following the isolation of subjects' DNA. The genotypes of *CYP2C9* *2 (rs1799853) and *3 (rs1057910) were determined using Taqman probe-based allele determination assays as previously described (Flora et al., 2017). The *CYP2C9* *1B genotype was characterized by -3089G>A (rs12782374) and -2663delTG (rs71486745) using assays described in a previous study (Chaudhry et al., 2010). All the genotyping assays were ordered from Applied Biosystems (Foster

City, California). It is worth mentioning that, although *1B genotypes may occur with multiple *CYP2C9* genotype backgrounds, the study presented here only involved *1B subjects with a wild-type *CYP2C9* background (*1/*1).

Written informed consent was required for subject enrollment. Subjects were eligible for enrollment if they were 18–60 years old, agreed to avoid the use of known *CYP2C9* or *CYP3A4* substrates, inhibitors, inducers, or activators, avoid the ingestion of grapefruit or grapefruit-related products, and avoid taking herbal medications or supplements from one week before the beginning of the study period to the end of the study period. Female subjects were eligible for enrollment only if they agreed to avoid conception during the study period. Smokers, subjects with abnormal renal/hepatic functions or abnormal capacity of blood coagulation, and subjects with an allergy to study drugs (warfarin, fluconazole, and rifampin) were excluded.

Study Design. The study was an open-label, multi-phase, and cross-over clinical pharmacogenetic study approved by the University of Minnesota's Institutional Review Board. The study design diagram is shown in Fig. 1. Twenty-nine healthy subjects with *CYP2C9* *1/*1 (*n* = 8), *CYP2C9* *1B/*1B (*n* = 5), *CYP2C9* *1/*3 (*n* = 9), *CYP2C9* *2/*3 (*n* = 3), and *CYP2C9* *3/*3 (*n* = 4) were enrolled in the study. The number of subjects enrolled for each *CYP2C9* genotype was determined to detect a 20% difference in S-warfarin 7-hydroxylation between subjects with *CYP2C9* *1/*1 and *1/*3 and achieve 80% statistical power (*P* < 0.05) (Kumar et al., 2008). Each subject went through three treatment periods during which warfarin was administered alone, with fluconazole, or with rifampin. For the first treatment period of study, each subject was administered a single 10-mg oral dose of warfarin (Jantoven; Upsher-Smith Laboratories, Maple Grove, Minnesota) after an overnight fast. Seven-milliliter blood samples were collected prior to the dose and at 2 hours, 6 hours, 1 day, 2 days, 3 days, 4 days, 5 days, 6 days, 7 days, 9 days, and 11 days for all subjects. Additional blood samples were collected at 13 days for subjects with *CYP2C9* *1/*3, *CYP2C9* *2/*3,* and *CYP2C9* *3/*3 and at 15 days for subjects with *CYP2C9* *2/*3 and *CYP2C9* *3/*3, as the half-life was expected to be longer in these subjects. Urine samples were collected over a 24-hour period on days 1, 4, 7, and 10 following warfarin administration. Each subject underwent a 7-day washout before entering the second treatment period of study. For the second treatment period, subjects were randomized to receive either 400 mg of fluconazole or 300 mg of rifampin orally once per day for 7 consecutive days as pretreatment to allow the fluconazole/rifampin interaction capacity to reach steady state. After pretreatment, a 10-mg oral dose of warfarin was administered, followed by the same blood and urine sampling scheme as the first treatment period. The administration of fluconazole or rifampin was continued until the end of sampling. Another 7-day washout period was required before entering the third treatment period. The design of the third period was the same as the second period, with subjects crossing over to the alternative interacting drug. S-warfarin and R-warfarin concentrations in blood and urine samples were analyzed by liquid chromatography/mass spectrometry as previously described (Miller et al., 2009; Flora et al., 2017).

PK Modeling. Dose-dependent changes in the volume of distribution have been observed in several preclinical and clinical studies with warfarin (Takada and Levy, 1979; Takada and Levy, 1980; King et al., 1995). To explain this unusual PK behavior exhibited by warfarin, Levy et al. proposed a complex PK phenomenon termed TMDD for the first time in 1994 (Levy, 1994) and successfully characterized warfarin clinical PK profiles with a TMDD model in 2003 (Levy et al., 2003). With the rapid development of therapeutic biologics in the early 2000s, the TMDD model has been widely used to explain the unusual PK nonlinearity in monoclonal antibodies (Luu et al., 2012; Vexler et al., 2013; Zheng et al., 2014). In addition, several studies published recently
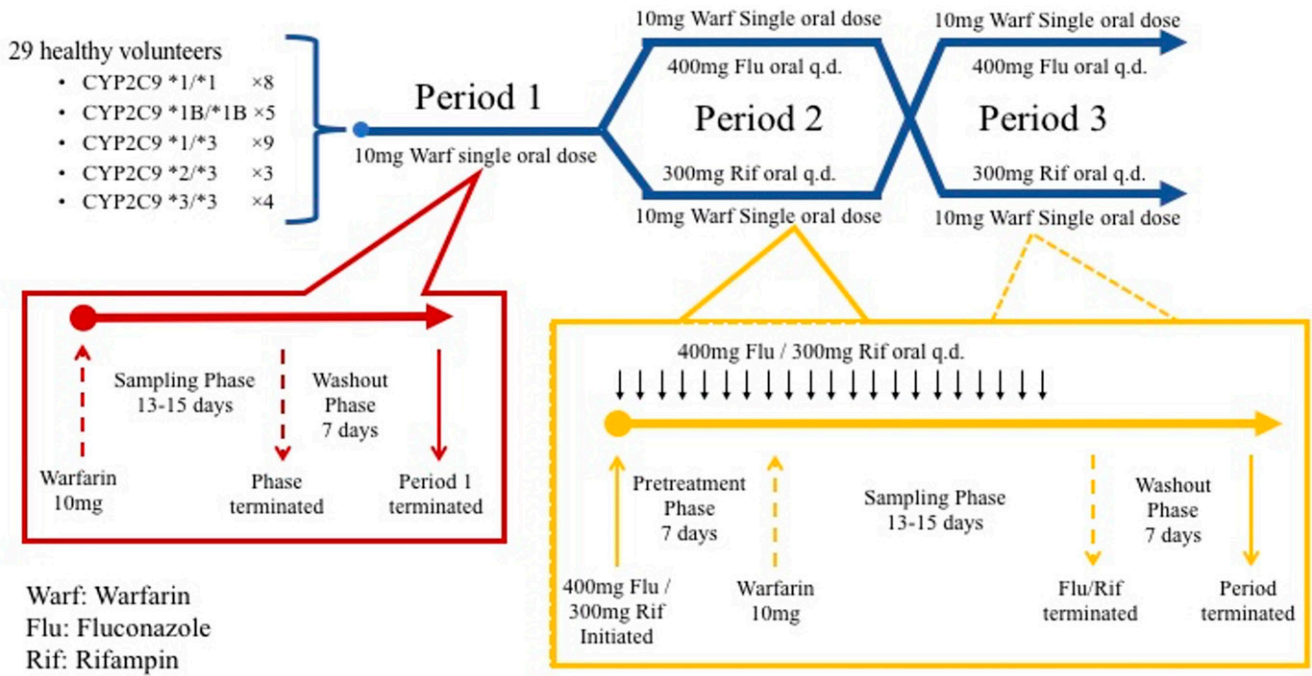
Fig. 1. Study Design Diagram. Each subject went through 3 study periods (upper dark blue section). Period 1 (red box), single 10 mg dose of warfarin. Periods 2 and 3 in crossover (yellow box), each subject was pretreated with either 400 of mg fluconazole or 300 mg of rifampin once daily for 7 consecutive days, followed by a single 10 mg dose of warfarin and continuous treatment with either 400 mg of fluconazole or 300 mg of rifampin once daily through the sampling phase. Notes: q.d.: Once daily.

readdressed the importance of the application of the TMDD models in small molecule drugs as well (Yamazaki et al., 2013; An et al., 2015; An, 2017).

The PK models used for fitting both S- and R-warfarin PK profiles are adapted from the TMDD model proposed for warfarin by Levy et al. (Levy et al., 2003; Bach et al., 2019) (Fig. 2). The model is described by eqs. 1–6 as shown below.

$$\frac{dA_{depot}}{dt} = -K_a \times A_{depot} \tag{1}$$

$$\frac{dA_{cent}}{dt} = K_a \times A_{depot} - CL \times \frac{A_{cent}}{V_C} - K_{on} \times A_{cent} \times A_R + K_{off} \times A_{DR}$$
$$\times V_C - CL_D \times \left(\frac{A_{cent}}{V_C} - \frac{A_{periph}}{V_P} \right) \tag{2}$$

$$\frac{dA_R}{dt} = -K_{on} \times \frac{A_{cent}}{V_C} \times A_R + K_{off} \times A_{DR} \tag{3}$$

$$\frac{dA_{DR}}{dt} = K_{on} \times \frac{A_{cent}}{V_C} \times A_R - K_{off} \times A_{DR} \tag{4}$$

$$\frac{dA_{periph}}{dt} = CL_D \times \left(\frac{A_{cent}}{V_C} - \frac{A_{periph}}{V_P} \right) \tag{5}$$
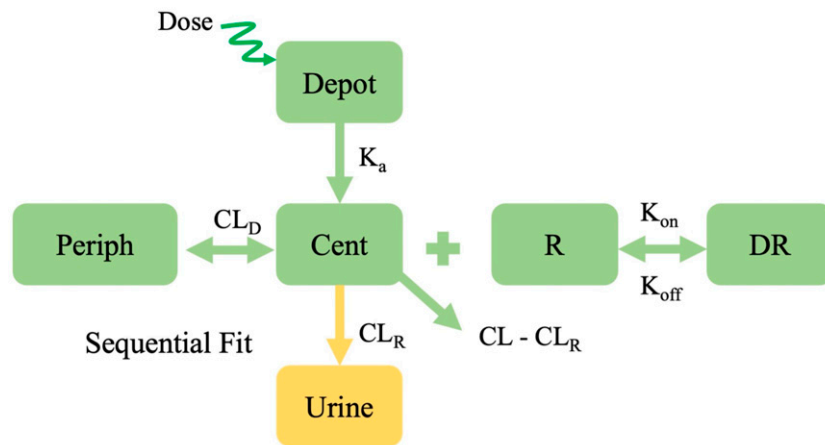
Fig. 2. PK model structure for S- and R-warfarin. Notes: Periph: peripheral; Cent: central.

$$\frac{dA_{urine}}{dt} = CL_r \times \frac{A_{cent}}{V_C} \quad (6)$$

where A_{depot}, A_{cent}, A_{periph}, and A_{urine} represent amounts in depot, central, peripheral, and urine compartments, respectively. A_R and A_{DR} represent concentrations in receptor and drug-receptor complex compartments, respectively. The definitions for other parameters are provided in Table 1 and 2.

The S- and R-warfarin data sets were modeled independently. For each enantiomer, plasma data from all three treatment periods were fit simultaneously. Eqs. 1–5 were used to estimate the parameters of each parent drug in plasma. A sequential modeling approach was applied for plasma and urine data. Once an adequate model with drug interaction parameters for plasma concentrations was determined, the empirical Bayes estimates of individual PK parameters were exported and merged into the data set. Eq. 6 was added, and the drug amounts from the 12 urine collections (4 collection times per treatment period) were fitted to estimate the renal CL (CL_R) portion of total CL. The bioavailability for each parent compound was assumed to be 1 for each dose during the study.

For the first treatment period, baseline plasma concentrations for S- and R- warfarin in central and peripheral compartments were assumed to be 0 given no detectable baseline warfarin concentrations at the beginning of first period. The baseline level of receptor compartment (R) was parameterized as baseline receptor level (R_{BL}) for estimation, and the baseline level of drug-receptor complex compartment (DR) was set as 0.

For the second and third treatment periods, warfarin concentrations were still occasionally measured after the 7-day washout period. The system was reinitialized at the beginning of subsequent treatments, but baseline concentrations for S- and R- warfarin in central and peripheral compartments were parameterized as BL and BL_P for estimation. Assuming a steady state at baseline for R (receptor) and DR (drug-receptor complex) compartments, eqs. 7–8 could be written as shown below.

$$A_R + A_{DR} = R_{BL} \quad (7)$$

$$K_{on} \times \frac{A_{cent}}{V_C} \times A_R - K_{off} \times A_{DR} = 0 \quad (8)$$

Given that the baseline concentration in the central compartment is parameterized as BL, eq. 8 could be written as eq. 9.

$$K_{on} \times BL \times A_R - K_{off} \times A_{DR} = 0 \quad (9)$$

With eq. 7 and eq. 9, A_R and A_{DR} baseline levels could be solved as shown by eqs. 10–11.

$$A_R = \frac{K_{off} \times R_{BL}}{K_{on} \times BL + K_{off}} \quad (10)$$

$$A_{DR} = \frac{K_{on} \times BL \times R_{BL}}{K_{on} \times BL + K_{off}} \quad (11)$$

Eqs. 10–11 were used for calculating baseline levels of R and DR compartments for study periods with fluconazole and rifampin (periods 2 and 3, respectively).

The covariate effects of *CYP2C9* genotypes and co-treatments were added on PK parameters using eq. 12 and eq. 13, respectively, as shown below.

$$TVP = TVP_{ref} \times P_{Geno} \, i \quad (12)$$

$$TVP = TVP_{ref} \times P_{TRT} \quad (13)$$

where (*TVP*: typical values of parameters; TVP_{ref}: typical values of parameters in reference groups; *P_Geno i*: *CYP2C9* genotype effect on parameters (i = 1, 2, 3, 4, and 5 represent *CYP2C9 *1/*1. *1B/*1B, *1/*3, *2/*3*, and *3/*3*, respectively); *P_TRT*: co-treatment effect on parameters (TRT: Flu: fluconazole, Rif: rifampin))

If an association between *P_TRT* and *CYP2C9* genotypes was detected visually, *CYP2C9* genotypes were added as a covariate on *P_TRT* using eq. 14.

$$P_{TRT} = P_{TRT} Geno \, i \quad (14)$$

where (*P_TRT_Geno i*: co-treatment effect on parameters for subjects with genotype i (i = 1, 2, 3, 4, and 5 represent *CYP2C9 *1/*1. *1B/*1B, *1/*3, *2/*3*, and *3/*3*, respectively))

A covariate introducing a 3.84 decrease in objective function values with one degree of freedom at an α level of 0.05 is considered to be statistically significant.

During model development, absorption rate constant (K_a) and BL_P were found to be estimated with inadequate precision. Since the warfarin is generally considered to be rapidly absorbed with almost complete bioavailability (Ufer, 2005), the bioavailability of warfarin was assumed to be 100%, and the K_a of both S- and R- warfarin were arbitrarily fixed as 2-hour^{-1}. BL_P was determined to fix as the closest positive integer value to the estimated values, which is 1 ug/L.

All the inter-individual variabilities (IIVs) were parameterized as log-normal distributions, as was inter-occasion variability (IOV) on R_{BL}. Residual unexplained variabilities (RUVs) were parameterized as proportional errors. All the IIVs and IOVs were assumed to be independent during plasma PK modeling so no off diagonal elements were estimated. In contrast, full omega matrices were estimated during urine PK modeling. MU-referencing is used for improving the efficiency of expectation-maximization (EM)-based optimization methods in NONMEM (Bauer, 2019). Fixed 1% IIVs were assumed for unwanted IIV terms to facilitate the optimization efficiency of EM-based methods (Chigutsa et al., 2017). Due to the existence of plasma concentrations below the quantification limit in R-warfarin PK data, the M3 method (Ahn et al., 2008; Bergstrand and Karlsson, 2009) suggested by Stuart Beal was used for fitting R-warfarin plasma PK profiles. All the modeling codes are provided in the supplemental materials (R- and S-warfarin plasma and urine PK model NONMEM codes).

Model Evaluation. The model fitting was evaluated by standard diagnostic plots and visual prediction checks (VPCs) with 200 simulations. The precision of parameter estimations was assessed by relative standard error (RSE) in the output and 95% confidence intervals (CIs) generated following sampling importance resampling (SIR) procedures (Dosne et al., 2016).

Model-Based Analysis on S-warfarin CL. Following the model development, the typical values of the effect of fluconazole and rifampin on S-warfarin CL (CL_Flu and CL_Rif) in subjects with different *CYP2C9* genotypes were exported. The percent changes in CL of S- and R-warfarin following the administration of warfarin together with fluconazole or rifampin is calculated using eq. 15 as shown below.

$$\% \, changes \, in \, CL = |CL_{TRT} - 100\%| \quad (15)$$

where (| *CL_TRT* – 100% |: absolute difference between co-treatment effects on CL and 100% (TRT: Flu: fluconazole, Rif: rifampin))

The 95% CIs were constructed with the RSE estimated from the covariance step by assuming a symmetrical normal distribution. The typical values and constructed 95% CIs were then plotted and compared.

Software. All the model fittings were performed using the EM-based algorithm, importance sampling with interaction, using MU-referencing and "AUTO=1" option, within NONMEM 7.4 (ICON Development Solutions, Ellicott City, Maryland) (Bauer, 2015). SIR and VPCs were performed with Perl-speaks-NONMEM (PsN 4.9.0, Uppsala, Sweden) within Pirana (Keizer et al., 2011). Plots were generated with R 3.6.3 (The R Foundation for Statistical Computing) and Rstudio 1.1.453 (Rstudio, Inc., Boston, Massachusetts).

TABLE 1
Summary of population PK parameter estimations for S-warfarin

Parameters	Definitions	Estimates (RSE)	SIR medians (95% CIs)	IIV/IOV Estimates (RSE)	IIV/IOV SIR medians (95% CIs)	Shrinkage	Units	Source
K_a	Absorption rate constant	2					/hour	Fixed
CL	Clearance for subjects with *CYP2C9 *1/*1* when warfarin is administered alone	0.260 (8%)	0.261 (0.221, 0.301)	22.9% (19%)	22.7% (17.5%, 27.8%)	1%	L/hour	Estimated by plasma model
V_C	Central compartment volume of distribution for subjects with *CYP2C9 *1/*1, *1B/*1B, *1/*3 and *3/*3*	5.00 (8%)	5.01 (4.42, 5.64)	21.4% (12%)	21.3% (15.8%, 26.1%)	6%	L	Estimated by plasma model
CL_D	Distribution clearance	1.25 (18%)	1.23 (0.94, 1.56)	21.7% (37%)	22.3% (5.8%, 34.8%)	41%	L/hour	Estimated by plasma model
V_P	Peripheral compartment volume of distribution	3.81 (8%)	3.80 (3.32, 4.24)	12.9% (54%)	13.5% (4.5%, 20.8%)	32%	L	Estimated by plasma model
K_{on}	Association rate constant between drug and receptor for subjects with *CYP2C9 *1/*1, *1B/*1B and *1/*3*	0.00494 (10%)	0.00500 (0.00402, 0.00590)	28.9% (44%)	30.5% (11.9%, 46.9%)	36%	L/(µg*hour)	Estimated by plasma model
K_{off}	Dissociation rate constant for drug-receptor complex	0.0405					/hour	Fixed (Levy et al., 2003)
R_{BL}	Baseline receptor level for subjects with *CYP2C9 *1/*1, *1B/*1B and *1/*3.*	182 (10%)	181 (155, 212)	18.9% (26%) (IIV) 19.5% (18%) (IOV)	19.6% (8.7%, 26.7%) 19.5% (14.1%, 24.6%)	30% 32% (Period1) 42% (Period2) 40% (Period3)	µg/L	Estimated by plasma model
CL_R	Renal clearance	0.00369 (5%)	0.00368 (0.00337, 0.00401)	20.1% (19%)	22.5% (15.5%, 29.2%)	11%	L/hour	Estimated by urine model
BL_P2	Period 2 baseline concentration in central compartment	3.65 (18%)	3.66 (2.53, 4.96)	106% (15%)	108% (74%, 153%)	9%	µg/L	Estimated by plasma model
BL_P3	Period 3 baseline concentration in central compartment	3.85 (29%)	3.89 (2.18, 5.97)	174% (40%)	172% (97%, 354%)	22%	µg/L	Estimated by plasma model
BL_P_P2	Period 2 baseline concentration in peripheral compartment	1					µg/L	Fixed
BL_P_P3	Period 3 baseline concentration in peripheral compartment	1					µg/L	Fixed
CL_Geno2	% CL for subjects with *CYP2C9 *1B/*1B* (reference *CYP2C9 *1/*1*)	88.5% (13%)	88.8% (69.0%, 112.0%)					Estimated by plasma model
CL_Geno3	% CL for subjects with *CYP2C9 *1/*3* (reference *CYP2C9 *1/*1*)	60.7% (11%)	61.0% (49.0%, 75.6%)					Estimated by plasma model
CL_Geno4	% CL for subjects with *CYP2C9 *2/*3* (reference *CYP2C9 *1/*1*)	27.7% (16%)	27.8% (19.6%, 35.8%)					Estimated by plasma model
CL_Geno5	% CL for subjects with *CYP2C9 *3/*3* (reference *CYP2C9 *1/*1*)	21.5% (14%)	21.7% (16.3%, 27.4%)					Estimated by plasma model
CL_Flu_Geno1	% of CL when administered with fluconazole for subjects with *CYP2C9 *1/*1*	30.5% (5%)	30.5% (27.8%, 33.4%)	12.5% (41%)	12.7% (8.2%, 18.4%)	25%		Estimated by plasma model
CL_Flu_Geno3	% of CL when administered with fluconazole for subjects with *CYP2C9 *1/*3*	35.2% (5%)	35.3% (32.1%, 38.4%)					Estimated by plasma model
CL_Flu_Geno4	% of CL when administered with fluconazole for subjects with *CYP2C9 *2/*3*	40.3% (8%)	40.4% (34.8%, 46.5%)					Estimated by plasma model

TABLE 1 *continued*

Parameters	Definitions	Estimates (RSE)	SIR medians (95% CIs)	IIV/IOV Estimates (RSE)	IIV/IOV SIR medians (95% CIs)	Shrinkage	Units	Source
CL_Flu_Geno5	% of CL when administered with fluconazole for subjects with *CYP2C9 *3/*3*	52.2% (7%)	52.4% (44.8%, 59.3%)					Estimated by plasma model
CL_Rif_Geno1	% of CL when administered with rifampin for subjects with *CYP2C9 *1/*1*	215% (4%)	215% (198%, 232%)	11.0% (20%)	11.3% (8.5%, 14.2%)	8%		Estimated by plasma model
CL_Rif_Geno2	% of CL when administered with rifampin for subjects with *CYP2C9 *1B/*1B*	211% (5%)	212% (190%, 233%)					Estimated by plasma model
CL_Rif_Geno3	% of CL when administered with rifampin for subjects with *CYP2C9 *1B/*1B*	219% (4%)	218% (203%, 235%)					Estimated by plasma model
CL_Rif_Geno4	% of CL when administered with rifampin for subjects with *CYP2C9 *1/*3*	298% (8%)	299% (253%, 347%)					Estimated by plasma model
CL_Rif_Geno5	% of CL when administered with rifampin for subjects with *CYP2C9 *2/*3*	293% (6%)	294% (261%, 330%)					Estimated by plasma model
V_C_Geno4	% of V_C for subjects with *CYP2C9 *2/*3* (reference all other genotypes)	55.6% (23%)	56.0% (37.0%, 76.3%)					Estimated by plasma model
K_{on}_Geno4	% of K_{on} for subjects with *CYP2C9 *2/*3* (reference **1/*1, *1B/*1B, *1/*3*)	83.7% (26%)	86.3% (49.1%, 131.3%)					Estimated by plasma model
K_{on}_Geno5	% of K_{on} for subjects with *CYP2C9 *3/*3* (reference **1/*1, *1B/*1B, *1/*3*)	51.8% (30%)	54.0% (29.9%, 83.1%)					Estimated by plasma model
R_{BL}_Geno4	% of R_{BL} for subjects with *CYP2C9 *2/*3* (reference **1/*1, *1B/*1B, *1/*3*)	251% (29%)	255% (152%, 385%)					Estimated by plasma model
R_{BL}_Geno5	% of R_{BL} for subjects with *CYP2C9 *3/*3* (reference **1/*1, *1B/*1B, *1/*3*)	189% (17%)	193% (134%, 258%)					Estimated by plasma model
CL_R_Flu	% of CL_R when administered with fluconazole	84.7% (5%)	85.4% (77.8%, 93.2%)	12.6% (48%)	17.2% (9.0%, 24.5%)	47%		Estimated by urine model
CL_R_Rif	% of CL_R when administered with rifampin	130% (6%)	132% (117%, 148%)	23.4 (25%)	27.4% (17.5%, 37.3%)	27%		Estimated by urine model
σwarf	RUV for warfarin alone period plasma	7.40% (5%)	7.43% (6.84%, 7.95%)					Estimated by plasma model
σwarf_Flu	RUV for warfarin + fluconazole period plasma	5.44% (5%)	5.49% (4.99%, 5.92%)					Estimated by plasma model
σwarf_Rif	RUV for warfarin + rifampin period plasma	9.20% (5%)	9.21% (8.54%, 9.93%)					Estimated by plasma model
σwarf_U	RUV for warfarin alone period urine	26.0% (8%)	27.8% (24.1%, 31.7%)					Estimated by urine model
σwarf_Flu_U	RUV for warfarin + fluconazole period urine	29.8% (10%)	29.9% (25.6%, 34.9%)					Estimated by urine model
σwarf_Rif_U	RUV for warfarin + rifampin period urine	26.0% (10%)	26.5% (22.4%, 31.4%)					Estimated by urine model

Notes: IIV and IOV terms are expressed as CV% ($\sqrt{e^{\sigma^2}-1}$); RUV terms are expressed as CV% ($\sqrt{\sigma^2}$).

Results

Data Summary. The demographic information for subjects involved in the study are provided in the supplementary materials (Supplemental Table 1). Data were available from 29 subjects that provided 957 S-warfarin plasma concentrations, all of which were above the lower limit of quantification (LLOQ, 0.67 ng/ml for S-warfarin). Those blood samples also provided 940 R-warfarin plasma concentrations. Of the 921 non-baseline R-warfarin plasma concentrations, 24 measurements (2.6%) were below the LLOQ (0.67 ng/ml for R-warfarin). Two hundred fifty-eight and 266 urine amount measurements were included in S- and R- warfarin urine PK model development, respectively. Not all subjects participated in three study periods; six subjects only participated in two study periods, and one subject only participated in one study period. These subjects were included in the analysis.

S-warfarin and R-warfarin plasma and urine PK profiles for subjects with different *CYP2C9* genotypes stratified by co-treatments are plotted in Fig. 3. The S-warfarin PK profiles in both plasma and urine under warfarin only treatment (Fig. 3, A and B left) clearly demonstrate *CYP2C9* genotype-dependent drug elimination. In contrast, R-warfarin plasma and urine PK profiles under warfarin only treatment indicate that the elimination of R-warfarin is independent of *CYP2C9* genotypes (Fig. 3, C and D left). Comparing S- and R-warfarin PK profiles under different co-treatments, the elimination appears to be slower and faster after the administration of fluconazole and rifampin, respectively.

S-Warfarin Model Parameters. The S-warfarin plasma PK model was able to converge after the inclusion of *CYP2C9* genotypes and co-treatments as covariates on CL. A TMDD model with a peripheral compartment (eqs. 1–5) was able to simultaneously characterize S-warfarin plasma PK profiles in the three treatment periods. Initially, the estimates K_a and the baseline concentration in the BL_p were estimated with inadequate precision (large %RSE). These parameters were then fixed as biologically plausible values as suggested in the Methods section. In addition, the estimations of association rate constant (K_{on}) and dissociation rate constant (K_{off}) exhibited a high degree of correlation and were initially estimated with poor precision. Literature reported K_{off} for racemic warfarin (Levy et al., 2003) was then fixed in the model, which enabled a precise estimation of K_{on}.

Subsequent visual inspections of the fluconazole effect on CL (CL_Flu) versus *CYP2C9* genotype plot (Figure S2 left) demonstrated the *CYP2C9* genotype-dependent changes in CL following the administration of fluconazole, with subjects possessing the *CYP2C9 *2 or *3* variants exhibiting smaller percentage changes. In contrast, visual inspection of the rifampin effect on CL (CL_Rif) versus *CYP2C9* genotypes (Figure S2 right) demonstrated *CYP2C9* genotype-dependent changes of CL following the administration of rifampin, with subjects possessing *CYP2C9 *2 or *3* variants exhibiting larger percentage changes. Thus, *CYP2C9* genotype was added as a covariate to CL_Flu and CL_Rif. Further visual inspections of the central volume of distribution (V_C), K_{on}, and R_{BL} versus *CYP2C9* genotype relationships showed that subjects with *CYP2C9 *2/*3* exhibit lower V_C, and subjects with *CYP2C9 *2/*3* and *CYP2C9 *3/*3* exhibit lower K_{on} and higher R_{BL}. These covariate effects were then added as fractions for estimation. The inclusion of IOV on R_{BL} significantly decreased the objective function value (-56.739).

The empirical Bayes estimates of individual PK parameters of S-warfarin were exported to the data set following the development of the plasma PK model. The urine PK model (eq. 6) for S-warfarin was developed subsequently with S-warfarin urine PK data. The final parameter estimations for S-warfarin are shown in Table 1.

R-Warfarin Model Parameters. Similar to the S-warfarin plasma PK model, the R-warfarin plasma PK model was able to converge after the inclusion of co-treatments as a covariate on CL. A TMDD model with a peripheral compartment (eqs.1–5) was able to sufficiently characterize the R-warfarin plasma PK profiles under different co-treatments simultaneously. The model parameters K_a, BL_p, and K_{off} were fixed as described for the S-warfarin PK model to avoid inadequate precision in model parameter estimations.

Visual inspection of model parameter versus *CYP2C9* genotype relationships found that subjects with *CYP2C9 *2/*3* and *CYP2C9 *3/*3* tended to have a lower and higher V_C, respectively. Subjects with *CYP2C9 *1/*3*, *CYP2C9 *2/*3* and *CYP2C9 *3/*3* tended to have a lower R_{BL}, and subjects with *CYP2C9 *2/*3* tend to have a higher CL_Rif. These covariate effects were added as a fractional multiplier for estimations. The inclusion of IOV on R_{BL} significantly decreased the objective function value (-63.796).

The empirical Bayes estimates of individual PK parameters of R-warfarin were exported to the data set following the development of the plasma PK model. Afterward, a urine PK model (eq.6) for R-warfarin was developed subsequently with R-warfarin urine PK data. The final parameter estimations for R-warfarin are shown in Table 2.

Model Evaluations. The VPCs for S-warfarin plasma and urine PK profiles and R-warfarin plasma and urine PK profiles stratified by both *CYP2C9* genotype and co-treatments are shown in Fig. 4 and 5. In general, the VPCs suggested all the models developed were able to explain the PK observations reasonably well. The RSE generated with covariance step and 95% CIs assessed by SIR suggested the model parameters were estimated with reasonable precisions (Table 1–2).

Standard diagnostic plots (Figures S3–S6: S-warfarin; Figure S8–S11: R-warfarin) stratified by either *CYP2C9* genotype or co-treatments and individual PK profile fittings (Figure S7: S-warfarin; Figure S12: R-warfarin) provide insufficient evidence to reject the models.

CYP2C9 Genotype-Dependent DDIs Exhibited by S-Warfarin. The parameter estimations from our model demonstrate the existence of the *CYP2C9* genotype-dependent changes in S-warfarin CL following the administration of fluconazole and rifampin (Fig. 6). The percentage inhibition in S-warfarin CL following the administration of fluconazole is largest in subjects with *CYP2C9 *1/*1*, followed by subjects with *CYP2C9 *1/*3*, *CYP2C9 *2/*3* and *CYP2C9 *3/*3*. In contrast, the percentage induction in S-warfarin CL following the administration of rifampin is much smaller in subjects with at least one copy of *CYP2C9 *1* or *1B* (*1/*1*, *1B/*1B*, *1/*3*) than subjects without *CYP2C9 *1 or *1B* (*2/*3*, *3/*3*).

Discussion

Numerous studies have been conducted to investigate the PK of warfarin since its introduction into clinical practice in the 1950s (Wen and Lee, 2013). Although *CYP2C9* genotype-dependent CL of S-warfarin has been shown in many studies (Hamberg et al., 2007; Gong et al., 2011; Flora et al., 2017; Xue et al., 2017), few have investigated the impact of the *CYP2C9* genotypes on warfarin DDIs. Taking advantage of PK data collected from a well-designed clinical warfarin DDI study, our study performed comprehensive population PK analysis on both S- and R-warfarin in plasma and urine, either administered alone or together with different co-medications. Our study confirmed the existence of *CYP2C9* genotype-dependent CL of S-warfarin, but not R-warfarin. More importantly, our study supports the existence of *CYP2C9* genotype-dependent DDIs of S-warfarin, the major active component in warfarin, when warfarin is administered with either fluconazole or rifampin. The study results indicate subjects with different *CYP2C9* genotypes

TABLE 2

Summary of population PK parameter estimations for R-warfarin

| Parameters	Definitions	Estimates (RSE)	SIR medians (95% CIs)	IIV/IOV Estimates (RSE)	IIV/IOV SIR medians (95% CIs)	Shrinkage	Units	Source
K_a	Absorption rate constant	2					/hour	Fixed
CL	Clearance when warfarin is administered alone	0.119 (5%)	0.119 (0.108, 0.131)	28.3% (12%)	29.1% (23.1%, 35.1%)	0%	L/hour	Estimated by plasma model
V_C	Central compartment volume of distribution for subjects with CYP2C9 *1/*1, *1B/*1B and *1/*3.	3.18 (8%)	3.19 (2.75, 3.65)	35.1% (11%)	38.1% (30.1%, 45.1%)	3%	L	Estimated by plasma model
CL_D	Distribution clearance	2.49 (2%)	2.46 (2.36, 2.56)				L/hour	Estimated by plasma model
V_P	Peripheral compartment volume of distribution	4.79 (1%)	4.79 (4.65, 4.93)				L	Estimated by plasma model
K_{on}	Association rate constant between drug and receptor	0.00137 (10%)	0.00139 (0.00116, 0.00163)	23.1% (64%)	29.1% (10.1%, 46.1%)	46%	L /(μg*hour)	Estimated by plasma model
K_{off}	Dissociation rate constant for drug-receptor complex	0.0405					/hour	Fixed (Levy et al., 2003)
R_{BL}	Baseline receptor level for subjects with CYP2C9 *1/*1, *1B/*1B.	188 (13%)	188 (154, 230)	15.6% (77%) (IIV); 36.0% (23%) (IOV)	23.1% (7.1%, 36.1%); 37.1% (27.1%, 50.1%)	57%; 29% (Period1) 44% (Period2) 45% (Period3)	μg/L	Estimated by plasma model
CL_R	Renal clearance	0.00436 (5%)	0.00433 (0.00396, 0.00480)	24.8% (18%)	27.4% (20.2%, 34.8%)	8%	L/hour	Estimated by urine model
BL_P2	Period 2 baseline concentration in central compartment	2.75 (23%)	2.82 (1.84, 4.01)	106% (33%)	121% (77%, 203%)	26%	μg/L	Estimated by plasma model
BL_P3	Period 3 baseline concentration in central compartment	1.97 (13%)	2.03 (1.57, 2.57)	29.3% (64%)	39.1% (20.1%, 63.1%)	63%	μg/L	Estimated by plasma model
BL_P_P2	Period 2 baseline concentration in peripheral compartment	1					μg/L	Fixed
BL_P_P3	Period 3 baseline concentration in peripheral compartment	1					μg/L	Fixed
CL_Flu	% of CL when administered with fluconazole	51.3% (4%)	51.1% (48.1%, 55.1%)	18.3% (13%)	19.1% (15.1%, 23.1%)	12%		Estimated by plasma model
CL_Rif	% of CL when administered with rifampin for subjects with CYP2C9 *1/*1, *1B/*1B, *2/*3 and *3/*3.	268% (3%)	268% (254%, 282%)	13.5% (14%)	14.1% (11.1%, 17.1%)	5%		Estimated by plasma model
CL_Rif_Geno4	% of CL when administered with rifampin for subjects with CYP2C9 *2/*3.	377% (10%)	380% (316%, 451%)					Estimated by plasma model
Vc_Geno4	% V_C for subjects with CYP2C9 *2/*3 (reference *1/*1, *1B/*1B, *1/*3)	71.1% (22%)	73.1% (48.1%, 104.1%)					Estimated by plasma model
Vc_Geno5	% V_C for subjects with CYP2C9 *3/*3 (reference *1/*1, *1B/*1B, *1/*3)	169% (19%)	175% (121%, 236%)					Estimated by plasma model
R_{BL}_Geno3	% R_{BL} for subjects with CYP2C9 *1/*3 (reference *1/*1, *1B/*1B)	47.9% (17%)	49.1% (36.1%, 65.1%)					Estimated by plasma model
R_{BL}_Geno4	% R_{BL} for subjects with CYP2C9 *2/*3 (reference *1/*1, *1B/*1B)	50.6% (22%)	52.1% (31.1%, 74.1%)					Estimated by plasma model
R_{BL}_Geno5	% R_{BL} for subjects with CYP2C9 *2/*3 (reference *1/*1, *1B/*1B)	21.0% (22%)	21.1% (14.1%, 30.1%)					Estimated by plasma model

TABLE 2 continued

Parameters	Definitions	Estimates (RSE)	SIR medians (95% CIs)	IIV/IOV Estimates (RSE)	IIV/IOV SIR medians (95% CIs)	Shrinkage	Units	Source
	% R_{BL} for subjects with *CYP2C9 *3/*3* (reference *1/*1, *1B/*1B*)							
CL_{R_Flu}	% of CL_R when administered with fluconazole	75.2% (5%)	75.6% (67.8%, 83.1%)	14.8% (58%)	20.5% (11.2%, 31.2%)	42%		Estimated by urine model
CL_{R_Rif}	% of CL_R when administered with rifampin	143% (8%)	143% (123%, 165%)	34.1% (22%)	39.5% (28.0%, 52.6%)	18%		Estimated by urine model
σ_{warf}	RUV for warfarin alone period plasma	7.37% (4%)	7.39% (6.82%, 8.05%)					Estimated by plasma model
σ_{warf_Flu}	RUV for warfarin + fluconazole period plasma	6.26% (5%)	6.29% (5.73%, 6.88%)					Estimated by plasma model
σ_{warf_Rif}	RUV for warfarin + rifampin period plasma	8.60% (5%)	8.59% (7.85%, 9.39%)					Estimated by plasma model
σ_{warf_U}	RUV for warfarin alone period urine	25.7% (8%)	27.4% (24.1%, 30.7%)					Estimated by urine model
$\sigma_{warf\_Flu\_U}$	RUV for warfarin + fluconazole period urine	31.1% (10%)	31.1% (26.9%, 36.3%)					Estimated by urine model
$\sigma_{warf\_Rif\_U}$	RUV for warfarin + rifampin period urine	26.8% (11%)	27.8% (23.4%, 33.0%)					Estimated by urine model

Notes: IIV and IOV terms are expressed as CV% $(\sqrt{e^{\sigma^2}-1})$; RUV terms are expressed as CV% $(\sqrt{\sigma^2})$.

potentially require different warfarin dose adjustments when warfarin is administered together with CYP inhibitors or inducers.

One of the obvious characteristics of small-molecule drugs exhibiting TMDD is the dose-dependent changes in apparent volume of distribution. This is caused by the saturation of the high-affinity, low-capacity binding sites at relatively high doses rather than low doses (An, 2017; Bach et al., 2019). This phenomenon was first reported by Dr. Gerhard Levy based on extensive preclinical studies conducted on warfarin PK (Takada and Levy, 1979; Takada and Levy, 1980). In fact, the term TMDD was first proposed by Dr. Levy in 1994 to explain the nonlinear PK behavior exhibited by small-molecule drugs, such as warfarin (Levy, 1994). Despite the relatively high prevalence of applying the TMDD models in characterizing the PK of large molecules, its usefulness in modeling small molecule compounds has gained recognition only recently (An, 2017). Indeed, with a linear compartmental PK model, we failed to fit either S- or R-warfarin plasma PK profiles under different co-treatments simultaneously (Figure S1, Supplemental Table 2). Interestingly, adequate fitting can be achieved with linear compartmental models if the PK profiles in each treatment period are fitted separately. However, a higher volume of distribution was estimated when warfarin is administered together with rifampin, and unrealistically long terminal half-lives were estimated. To some extent, this is consistent with the dose-dependent changes in volume of distribution shown by an early warfarin clinical PK study, in which a higher volume of distribution is shown for subjects with lower doses (King et al., 1995). We suspected that when either a low dose of warfarin is administered or warfarin is cleared faster following the co-administration of a CYP inducer, the unsaturation of the high-affinity, low-capacity binding sites causes a higher apparent volume of distribution to be estimated. Additionally, a prolonged terminal phase was commonly observed for small-molecule drugs exhibiting TMDD (An et al., 2015). The back-extrapolation to the intercept of the prolonged terminal phase normally converges to the same concentration regardless of dose (An, 2017; Bach et al., 2019). This is because the high-affinity binding between drugs and binding sites makes the dissociation between them extremely slow, which becomes the rate-limiting step for drug elimination when drug concentration in the plasma is low (Bach et al., 2019).

Although the phenomenon of TMDD for certain small molecule drugs dates back many years, the application of TMDD models in modeling warfarin PK is rare (Levy, 1994; Mager and Jusko, 2001). This is not surprising given the difficulties in study design to enable observation of the TMDD type of PK behavior in small-molecule drugs, such as like warfarin. Although the unsaturation of binding sites at relatively low doses causes a higher volume of distribution to be estimated, following repeated low doses, the binding sites are generally saturated, which leads to observations of linear PK (An, 2017; Bach et al., 2019). Thus, a single-dose study with different dosage levels is normally required to fit a TMDD model adequately. In addition, to capture the prolonged terminal phase, a relatively long follow up time is also required. Given that many studies were conducted with patients taking warfarin on a regular basis or relatively short follow-up time following single dose of administration (Hamberg et al., 2007; Xue et al., 2017), it is not surprising that linear compartmental models are still widely used for modeling warfarin PK in these studies. Additionally, TMDD models are known to be overparametrized and are difficult to converge (Gibiansky et al., 2008). Indeed, a full TMDD model was tested initially. However, several model parameters, such as K_{on} and K_{off}, were highly correlated and cannot be estimated with adequate precision. Thus, K_{off} values of warfarin were fixed to the literature reported value (Levy et al., 2003) and only K_{on} values were estimated. While this approach is sufficient to overcome the difficulties we encountered, several approximation methods of TMDD, such as quasi-equilibrium, could be used if reliable K_{off}
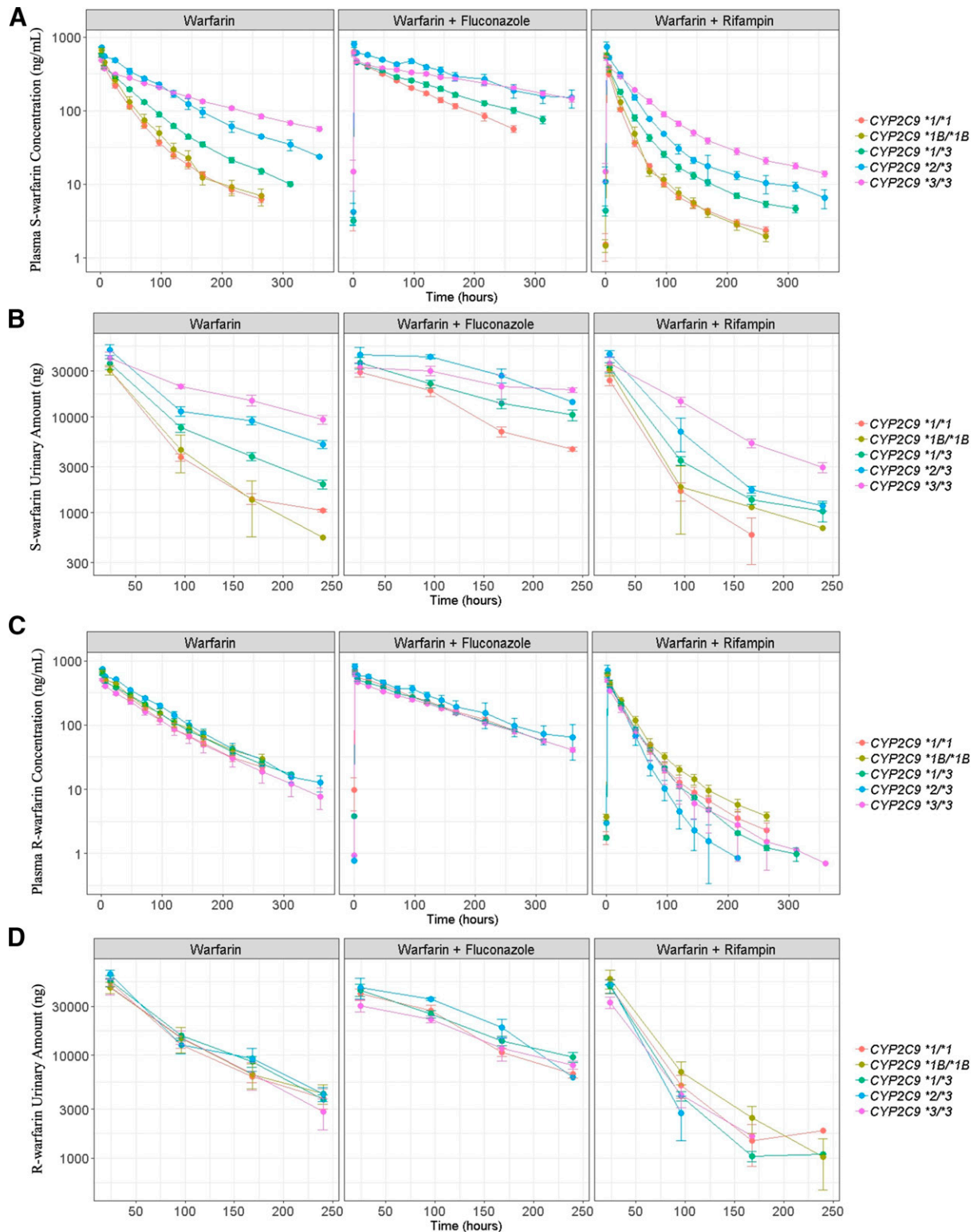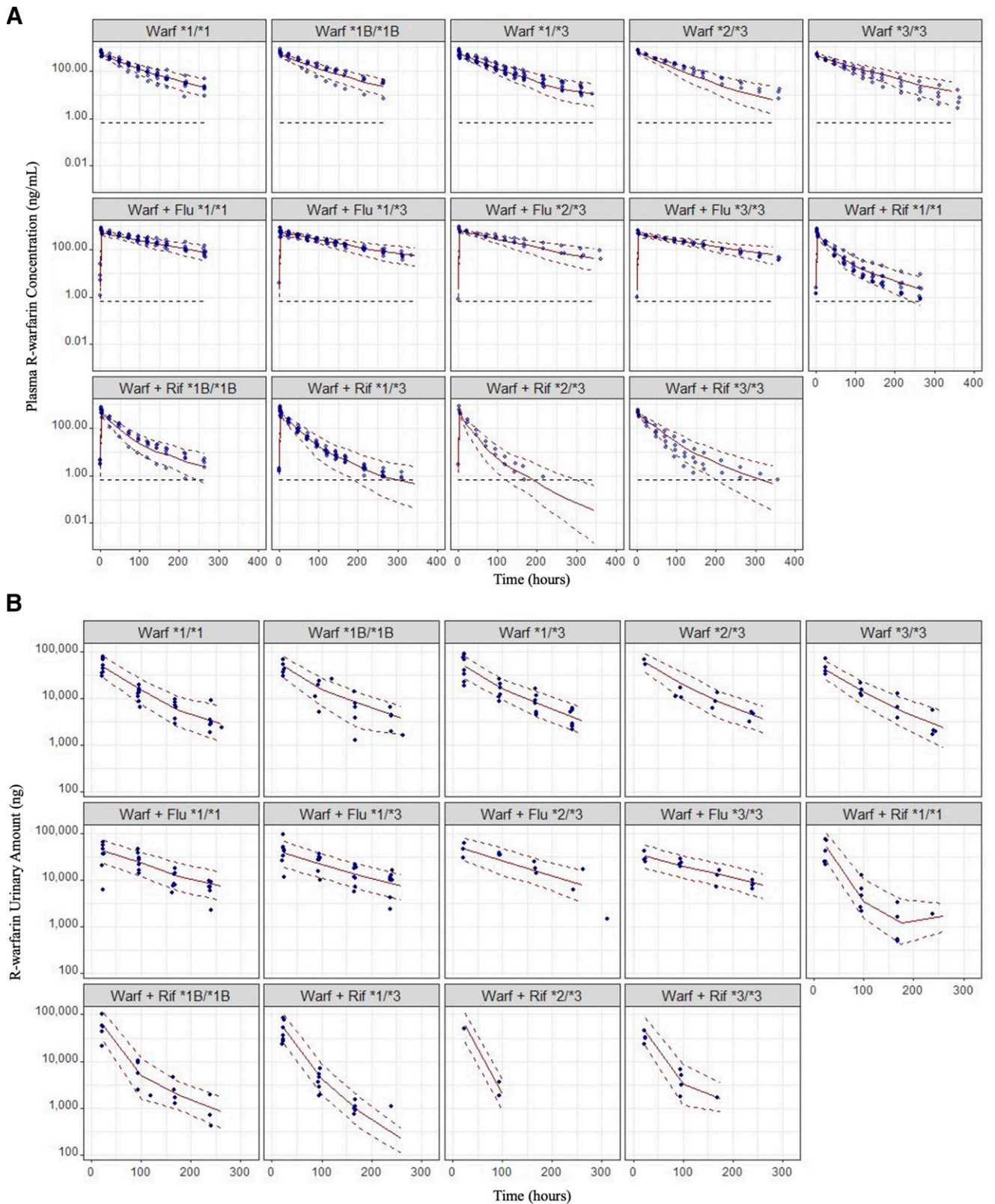
Fig. 3. PK profiles for S-warfarin in plasma (A) and urine (B) and R-warfarin in plasma (C) and urine (D). All the PK profiles are stratified by co-treatments. Colors represent different *CYP2C9* genotypes as shown in figure legends. Plots are on log scales. Points represent mean and error bars represent 95% confidence intervals.

values are not available (Mager and Krzyzanski, 2005; Gibiansky et al., 2008). During the model development, K_a and BL_P were estimated with inadequate precision and were also fixed in the model as 2 hour^{-1} and

1 µg/L, respectively. Similar values of K_a were used for developing other S- and R-warfarin PK models (Hamberg et al., 2007; Xue et al., 2017). BL_P was determined to fix as the closest positive integer value to
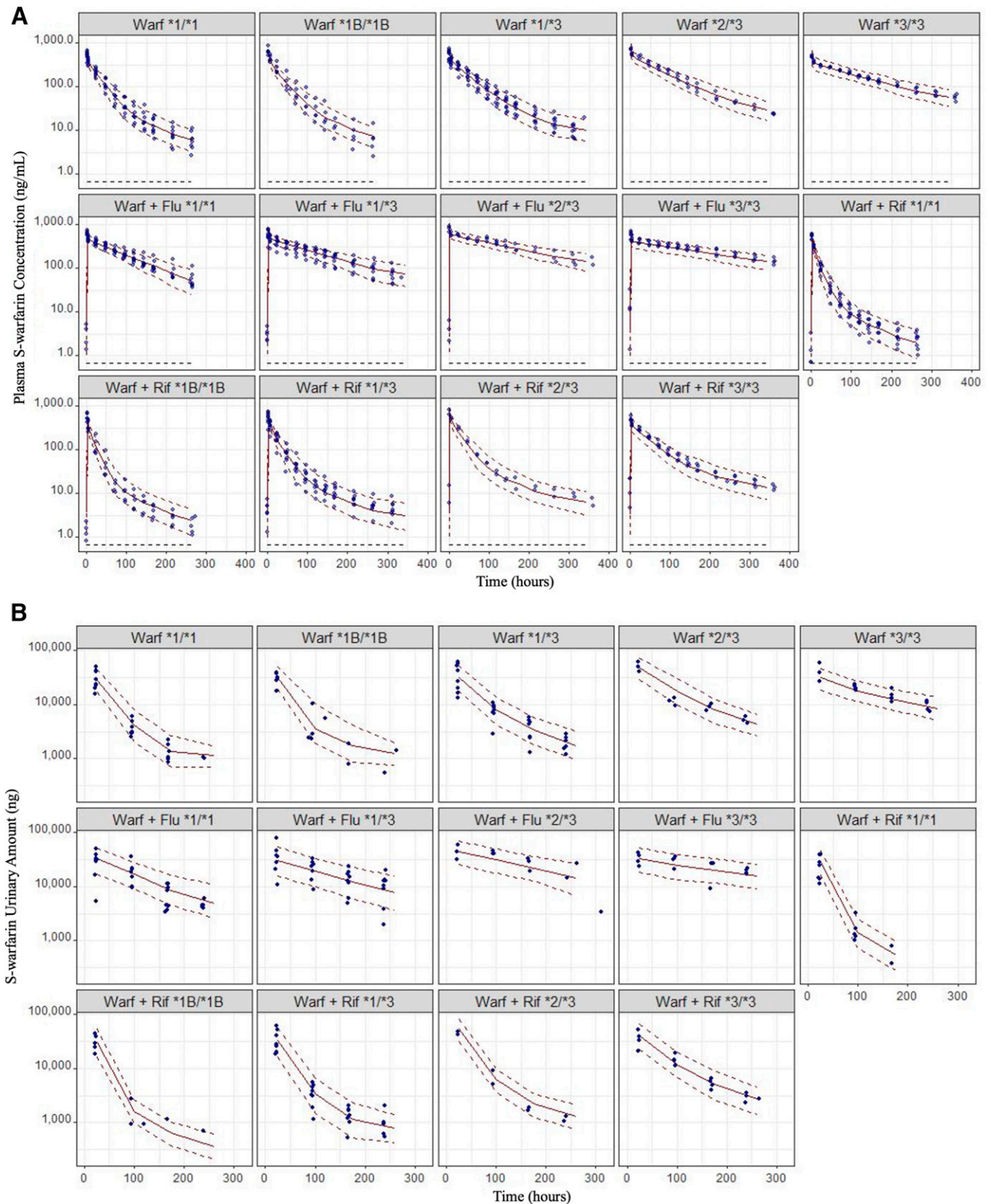
Fig. 4. VPCs for S-warfarin PK profiles in plasma (A) and urine (B). Blue dots represent the observations. Red solid lines represent the medians of model predicted concentrations. The upper and lower red dashed lines represent the 10th and 90th percentiles of the model predicted concentrations, respectively. The figure is stratified by genotypes and co-treatments. The black dashed lines represent the LLOQ for S-warfarin (0.67 ng/ml). No observations were collected from *CYP2C9 *1B/*1B* subjects and treated with warfarin plus fluconazole. Note: Warf: warfarin; Flu: fluconazole; Rif: rifampin; *1/*1: *CYP2C9 *1/*1*; *1B/*1B: *CYP2C9 *1B/*1B*; *1/*3: *CYP2C9 *1/*3*; *2/*3: *CYP2C9 *2/*3*; *3/*3: *CYP2C9 *3/*3*.

Fig. 5. VPCs for R-warfarin PK profiles in plasma (A) and urine (B). Blue dots represent the observations. Red solid lines represent the medians of model predicted concentrations. The upper and lower red dashed lines represent the 10th and 90th percentiles of the model predicted concentrations, respectively. The figure is stratified by genotypes and co-treatments. The black dashed lines represent the LLOQ for R-warfarin (0.67 ng/ml). No observations were collected from *CYP2C9 *1B/*1B* subjects and treated with warfarin plus fluconazole. Note: Warf: warfarin; Flu: fluconazole; Rif: rifampin; *1/*1: *CYP2C9 *1/*1*; *1B/*1B: *CYP2C9 *1B/*1B*; *1/*3: *CYP2C9 *1/*3*; *2/*3: *CYP2C9 *2/*3*; *3/*3: *CYP2C9 *3/*3*.
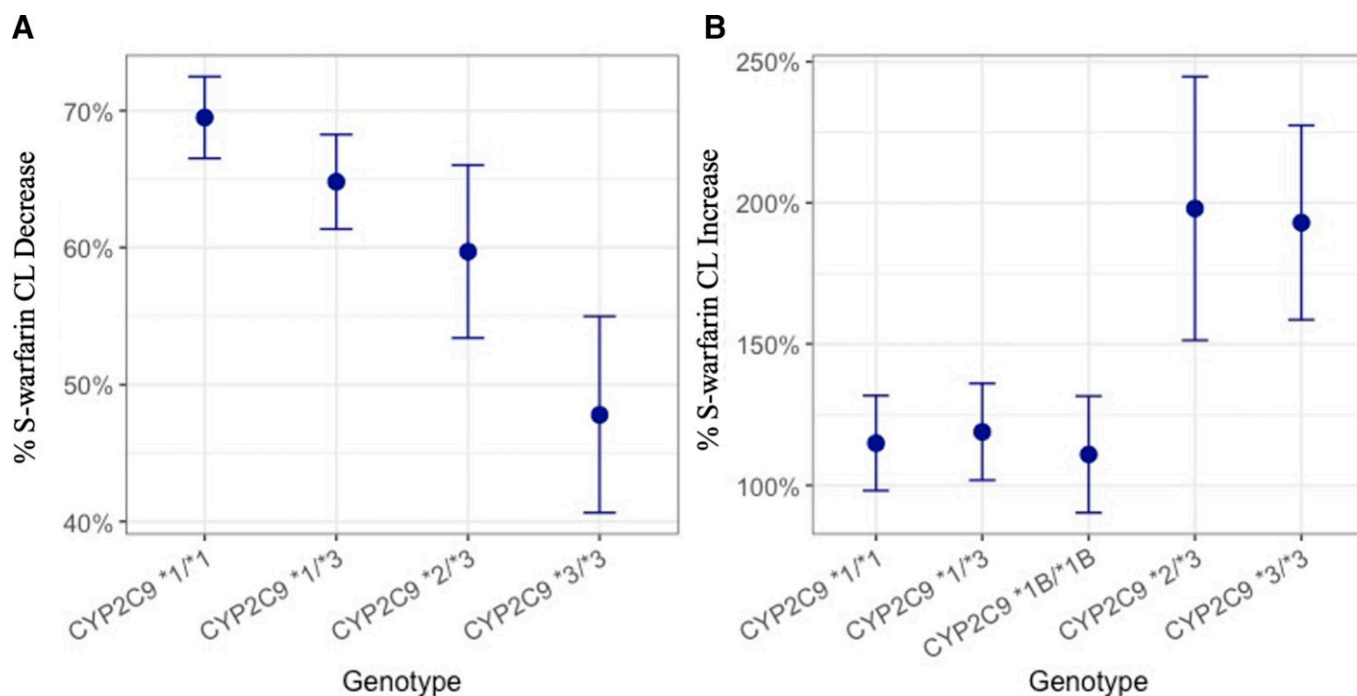
Fig. 6. Genotype-dependent CL changes of S-warfarin following the administration of fluconazole (A) and rifampin (B). The dots and error bars represent the typical values and 95% CIs, respectively. The 95% CIs are constructed with RSE as shown in Table 1 assuming a symmetric normal distribution.

the estimated values, which is 1 ug/L. Given that the initial concentration of both S- and R-warfarin can reach as high as 1000 ug/L and the scale of V_C and V_P are similar, a 1 ug/L BL_P is highly unlikely to be impactful (Table 1).

Polypharmacy is more prevalent in older individuals (Maher et al., 2014). A better understanding in CL changes of warfarin, especially when warfarin is administered together with either CYP inhibitors or inducers, is critical to adjust warfarin doses rationally for patients under polypharmacy. Interestingly, our study shows subjects with *CYP2C9 *2* or *3* alleles experience a smaller and larger percentage of CL changes for S-warfarin following the administration of fluconazole and rifampin, respectively. Since S-warfarin is the more active enantiomer in the racemate, smaller dose adjustments should be made for subjects with *CYP2C9 *2* or *3* variants, when they take warfarin together with fluconazole. In contrast, larger dosing adjustments should be made for these subjects when they take warfarin together with rifampin. It is also worth mentioning that both fluconazole and rifampin are non-specific CYP inhibitors and inducers, respectively. The differences in the percentage of fluconazole inhibition or rifampin induction in S-warfarin CL for patients with different *CYP2C9* genotypes might indicate certain CYP enzymes involved in warfarin elimination are potentially more inhibitable or inducible than others. The warfarin metabolic profile changes following the administration of CYP inhibitors or inducers in subjects with different *CYP2C9* genotypes are evaluated in our companion study, in which the PK profiles of 10 warfarin metabolites under different treatment conditions are modeled on the basis of the parent compound models presented here (Cheng et al., concurrently published). The elucidation of metabolic profile changes of warfarin, following the administration of non-specific CYP inhibitors or inducers, is not only useful in gaining more mechanistic insights behind the *CYP2C9* genotype-dependent DDIs exhibited by S-warfarin, but also valuable to inform the DDIs of other drugs which undergo similar metabolic pathways.

Although the impact of *CYP2C9* alone on warfarin therapeutic outcomes, such as international normalized ratio (INR), was well recognized (Ufer, 2005), the impact of *CYP2C9* on warfarin DDIs in the context of therapeutic outcomes has rarely been investigated. Hamberg et al. developed a PK-PD model for warfarin (Hamberg et al., 2007) and demonstrated that the EC_{50} of INR responses to S-warfarin concentrations vary across different vitamin K epoxide reductase complex subunit 1 (*VKORC1*) genotypes (GG: 4.61 mg/L, GA: 3.20 mg/L, AA: 2.20 mg/L), and the IIV of PD parameters are relatively high. It is likely the PD variability of warfarin overwhelms the PK variability of warfarin, which makes the PK variability of warfarin less of a concern when monitoring INR. Nevertheless, many studies have suggested that *CYP2C9* and *VKORC1* genetic polymorphisms together can account for up to 30% of total variability in warfarin doses, in which *VKORC1* and *CYP2C9* genetic polymorphism alone can account for 25% and 9%, respectively (Limdi et al., 2008; Fung et al., 2012). Furthermore, a recent clinical case report showed that a subject with *CYP2C9 *3/*3* and *VKORC1 GA* mutations required a larger magnitude of warfarin dose adjustments, while warfarin was treated together with rifampin (Salem et al., 2021). The conclusion of the case report is consistent with our findings to some extent. Thus, the impact of *CYP2C9* genotype-dependent DDIs on the therapeutic outcomes of warfarin is ambiguous, which may warrant further investigations given the narrow therapeutic index of warfarin. Although the dosing of warfarin remains challenging, substantial progress has been made using a model-informed approach. For example, Wright et al. proposed warfarin dose individualization under a Bayesian framework which allows the maintenance of the steady state INR 65% to 80% of the time within the therapeutic index of warfarin when more than 3 INR measurements are available (Wright and Duffull, 2013). The incorporation of the TMDD mechanism presented in this study may provide more mechanistic insights about warfarin dispositions and further improves the warfarin dosing in scenarios such as warfarin treatment initialization and discontinuation.

Limitations were noted in the present study. For example, several covariate effects, such as the *CYP2C9* effects on K_{on}, V_C, and R_{BL}, are lacking a mechanistic basis, although they are statistically significant. Indeed, the original objective of this clinical study is to characterize and quantify the *CYP2C9* genotype-dependent DDIs of warfarin. Based on the purpose of the study, a small number of subjects ($n = 29$) was enrolled and a limited number of covariates was collected. During the model development, we found that the PK variabilities cannot be fully accounted for by the effect of *CYP2C9* and drug interactions on CL. This is anticipated given that the PK of warfarin is notoriously known to be impacted by many factors, such as diet and drug transporter functions, that were not collected in the current study (Ovesen et al., 1988; Bi et al., 2018). Thus, although lacking a mechanistic basis, these covariate effects were still added to account for some observed PK variability so that the *CYP2C9* genotype-dependent DDIs of warfarin can be better characterized. However, future clinical studies with more covariates collected may be warranted to validate these covariate effects.

In summary, we conducted a comprehensive nonlinear mixed effect PK analysis to evaluate the impact of *CYP2C9* genotypes on both S- and R-warfarin DDIs. Our study found that subjects with different *CYP2C9* genotypes experience differences in S-warfarin CL changes following the administration of CYP inhibitors or inducers, indicating that *CYP2C9* genotype-dependent warfarin dose adjustments are potentially required. In the future, connecting with literature reported PD models, the PK models presented in this study may be useful in informing dose adjustments on the basis of therapeutic outcome predictions. Thus, the models presented in this study may serve as a valuable tool for optimizing warfarin dosing adjustments in a polypharmacy setting.

Authorship Contributions

Participated in research design: Cheng, Flora, Rettie, Brundage, Tracy.

Conducted experiments: Flora, Rettie, Tracy.

Performed data analysis: Cheng, Brundage.

Wrote or contributed to the writing of the manuscript: Cheng, Flora, Rettie, Brundage, Tracy.

Citation of meeting abstracts: Cheng S., Flora D.R., Tracy T. S., Rettie A.E., Brundage R.C. Genotype-Dependent Changes in Warfarin Clearance upon Co-administration of an Inhibitor (fluconazole) and an inducer (rifampin): A Model-based Analysis. American Conference of Pharmacometrics (ACOP) 11

References

Ahn JE, Karlsson MO, Dunne A, and Ludden TM (2008) Likelihood based approaches to handling data below the quantification limit using NONMEM VI. *J Pharmacokinet Pharmacodyn* **35**:401–421.

An G (2017) Small-Molecule Compounds Exhibiting Target-Mediated Drug Disposition (TMDD): A Minireview. *J Clin Pharmacol* **57**:137–150.

An G, Liu W, and Dutta S (2015) Small-molecule compounds exhibiting target-mediated drug disposition - A case example of ABT-384. *J Clin Pharmacol* **55**:1079–1085.

Asiimwe IG, Zhang EJ, Osanlou R, Jorgensen AL, and Pirmohamed M (2021) Warfarin dosing algorithms: A systematic review. *Br J Clin Pharmacol* **87**:1717–1729.

Bach T, Jiang Y, Zhang X, and An G (2019) General Pharmacokinetic Features of Small-Molecule Compounds Exhibiting Target-Mediated Drug Disposition (TMDD): A Simulation-Based Study. *J Clin Pharmacol* **59**:394–405.

Barnes GD, Lucas E, Alexander GC, and Goldberger ZD (2015) National Trends in Ambulatory Oral Anticoagulant Use. *Am J Med* **128**:1300–5.e2.

Bauer RJ(2015) NONMEM Users Guide: Introduction to NONMEM 7.3.0, in, *ICON plc.* Gaithersburg, Maryland.

Bauer RJ (2019) NONMEM Tutorial Part II: Estimation Methods and Advanced Examples. *CPT Pharmacometrics Syst Pharmacol.* **218**:538–556.

Bergstrand M and Karlsson MO (2009) Handling data below the limit of quantification in mixed effect models. *AAPS J* **11**:371–380.

Bi YA, Lin J, Mathialagan S, Tylaska L, Callegari E, Rodrigues AD, and Varma MVS (2018) Role of Hepatic Organic Anion Transporter 2 in the Pharmacokinetics of R- and S-Warfarin: In Vitro Studies and Mechanistic Evaluation. *Mol Pharm* **15**:1284–1295.

Breckenridge A, Orme M, Wesseling H, Lewis RJ, and Gibbons R (1974) Pharmacokinetics and pharmacodynamics of the enantiomers of warfarin in man. *Clin Pharmacol Ther* **15**:424–430.

Chaudhry AS, Urban TJ, Lamba JK, Birnbaum AK, Remmel RP, Subramanian M, Strom S, You JH, Kasperaviciute D, Catarino CB et al. (2010) CYP2C9*1B promoter polymorphisms, in linkage with CYP2C19*2, affect phenytoin autoinduction of clearance and maintenance dose. *J Pharmacol Exp Ther* **332**:599–611.

Cheng S, Flora DR, Tracy TS, Rettie AE, and Brundage RC (concurrently published) Pharmacokinetic Modeling of Warfarin II – Model-based Analysis of Warfarin Metabolites following Warfarin Administered either Alone or Together with Fluconazole or Rifampin. *Drug Metab and Disp* **50**.

Chigutsa E, Long AJ, and Wallin JE (2017) Exposure-Response Analysis of Necitumumab Efficacy in Squamous Non-Small Cell Lung Cancer Patients. *CPT Pharmacometrics Syst Pharmacol* **6**:560–568.

Dosne AG, Bergstrand M, Harling K, and Karlsson MO (2016) Improving the estimation of parameter uncertainty distributions in nonlinear mixed effects models using sampling importance resampling. *J Pharmacokinet Pharmacodyn* **43**:583–596.

Finkelman BS, Gage BF, Johnson JA, Brensinger CM, and Kimmel SE (2011) Genetic warfarin dosing: tables versus algorithms. *J Am Coll Cardiol* **57**:612–618.

Flora DR, Rettie AE, Brundage RC, and Tracy TS (2017) CYP2C9 Genotype-Dependent Warfarin Pharmacokinetics: Impact of CYP2C9 Genotype on R- and S-Warfarin and Their Oxidative Metabolites. *J Clin Pharmacol* **57**:382–393.

Fung E, Patsopoulos NA, Belknap SM, O'Rourke DJ, Robb JF, Anderson JL, Shworak NW, and Moore JH (2012) Effect of genetic variants, especially CYP2C9 and VKORC1, on the pharmacology of warfarin. *Semin Thromb Hemost* **38**:893–904.

Gage BF, Eby C, Johnson JA, Deych E, Rieder MJ, Ridker PM, Milligan PE, Grice G, Lenzini P, Rettie AE et al. (2008) Use of pharmacogenetic and clinical factors to predict the therapeutic dose of warfarin. *Clin Pharmacol Ther* **84**:326–331.

Gibiansky L, Gibiansky E, Kakkar T, and Ma P (2008) Approximations of the target-mediated drug disposition model and identifiability of model parameters. *J Pharmacokinet Pharmacodyn* **35**:573–591.

Gong IY, Schwarz UI, Crown N, Dresser GK, Lazo-Langner A, Zou G, Roden DM, Stein CM, Rodger M, Wells PS et al. (2011) Clinical and genetic determinants of warfarin pharmacokinetics and pharmacodynamics during treatment initiation. *PLoS One* **6**:e27808.

Hamberg AK, Dahl ML, Barban M, Scordo MG, Wadelius M, Pengo V, Padrini R, and Jonsson EN (2007) A PK-PD model for predicting the impact of age, CYP2C9, and VKORC1 genotype on individualization of warfarin therapy. *Clin Pharmacol Ther* **81**:529–538.

Hart RG, Pearce LA, and Aguilar MI (2007) Meta-analysis: antithrombotic therapy to prevent stroke in patients who have nonvalvular atrial fibrillation. *Ann Intern Med* **146**:857–867.

Kawai VK, Cunningham A, Vear SI, Van Driest SL, Oginni A, Xu H, Jiang M, Li C, Denny JC, Shaffer C et al. (2014) Genotype and risk of major bleeding during warfarin treatment. *Pharmacogenomics* **15**:1973–1983.

Keizer RJ, van Benten M, Beijnen JH, Schellens JH, and Huitema AD (2011) Piraña and PCluster: a modeling environment and cluster infrastructure for NONMEM. *Comput Methods Programs Biomed* **101**:72–79.

Kimmel SE, French B, Kasner SE, Johnson JA, Anderson JL, Gage BF, Rosenberg YD, Eby CS, Madigan RA, McBane RB et al.; COAG Investigators (2013) A pharmacogenetic versus a clinical algorithm for warfarin dosing. *N Engl J Med* **369**:2283–2293.

King SY, Joslin MA, Raudibaugh K, Pieniaszek Jr HJ, and Benedek IH (1995) Dose-dependent pharmacokinetics of warfarin in healthy volunteers. *Pharm Res* **12**:1874–1877.

Kumar V, Brundage RC, Oetting WS, Leppik IE, and Tracy TS (2008) Differential genotype dependent inhibition of CYP2C9 in humans. *Drug Metab Dispos* **36**:1242–1248.

Levy G (1994) Pharmacologic target-mediated drug disposition. *Clin Pharmacol Ther* **56**: 248–252.

Levy G, Mager DE, Cheung WK, and Jusko WJ (2003) Comparative pharmacokinetics of coumarin anticoagulants L: Physiologic modeling of S-warfarin in rats and pharmacologic target-mediated warfarin disposition in man. *J Pharm Sci* **92**:985–994.

Lewis RJ, Trager WF, Chan KK, Breckenridge A, Orme M, Roland M, and Schary W (1974) Warfarin. Stereochemical aspects of its metabolism and the interaction with phenylbutazone. *J Clin Invest* **53**:1607–1617.

Limdi NA, Arnett DK, Goldstein JA, Beasley TM, McGwin G, Adler BK, and Acton RT (2008) Influence of CYP2C9 and VKORC1 on warfarin dose, anticoagulation attainment and maintenance among European-Americans and African-Americans. *Pharmacogenomics* **9**:511–526.

Luu KT, Bergqvist S, Chen E, Hu-Lowe D, and Kraynov E (2012) A model-based approach to predicting the human pharmacokinetics of a monoclonal antibody exhibiting target-mediated drug disposition. *J Pharmacol Exp Ther* **341**:702–708.

Mager DE and Jusko WJ (2001) General pharmacokinetic model for drugs exhibiting target-mediated drug disposition. *J Pharmacokinet Pharmacodyn* **28**:507–532.

Mager DE and Krzyzanski W (2005) Quasi-equilibrium pharmacokinetic model for drugs exhibiting target-mediated drug disposition. *Pharm Res* **22**:1589–1596.

Maher RL, Hanlon J, and Hajjar ER (2014) Clinical consequences of polypharmacy in elderly. *Expert Opin Drug Saf* **13**:57–65.

Mak M, Lam C, Pineda SJ, Lou M, Xu LY, Meeks C, Lin C, Stone R, Rodgers K, and Mitani G (2019) Pharmacogenetics of Warfarin in a Diverse Patient Population. *J Cardiovasc Pharmacol Ther* **24**:521–533.

Miller GP, Jones DR, Sullivan SZ, Mazur A, Owen SN, Mitchell NC, Radominska-Pandya A, and Moran JH (2009) Assessing cytochrome P450 and UDP-glucuronosyltransferase contributions to warfarin metabolism in humans. *Chem Res Toxicol* **22**:1239–1245.

O'Reilly RA (1974) Studies on the optical enantiomorphs of warfarin in man. *Clin Pharmacol Ther* **16**:348–354.

Ovesen L, Lyduch S, and Idorn ML (1988) The effect of a diet rich in brussels sprouts on warfarin pharmacokinetics. *Eur J Clin Pharmacol* **34**:521–523.

Rettie AE, Korzekwa KR, Kunze KL, Lawrence RF, Eddy AC, Aoyama T, Gelboin HV, Gonzalez FJ, and Trager WF (1992) Hydroxylation of warfarin by human cDNA-expressed cytochrome P-450: a role for P-4502C9 in the etiology of (S)-warfarin-drug interactions. *Chem Res Toxicol* **5**:54–59.

Rettie AE and Tai G (2006) The pharmacogenomics of warfarin: closing in on personalized medicine. *Mol Interv* **6**:223–227.

Salem M, Eljilany I, El-Bardissy A, and Elewa H (2021) Genetic Polymorphism Effect on Warfarin-Rifampin Interaction: A Case Report and Review of Literature. *Pharm Genomics Pers Med* **14**: 149–156.

Takada K and Levy G (1979) Comparative pharmacokinetics of coumarin anticoagulants XLIII: Concentration-dependent hepatic uptake of warfarin in rats. *J Pharm Sci* **68**:1569–1571.

Takada K and Levy G (1980) Comparative pharmacokinetics of coumarin anticoagulants XLIV: Dose-dependent pharmacokinetics of warfarin in rats. *J Pharm Sci* **69**:9–14.

Takahashi H and Echizen H (2001) Pharmacogenetics of warfarin elimination and its clinical implications. *Clin Pharmacokinet* **40**:587–603.

Ufer M (2005) Comparative pharmacokinetics of vitamin K antagonists: warfarin, phenprocoumon and acenocoumarol. *Clin Pharmacokinet* **44**:1227–1246.

Veenstra DL, Blough DK, Higashi MK, Farin FM, Srinouanprachan S, Rieder MJ, and Rettie AE (2005) CYP2C9 haplotype structure in European American warfarin patients and association with clinical outcomes. *Clin Pharmacol Ther* **77**:353–364.

Vexler V, Yu L, Pamulapati C, Garrido R, Grimm HP, Sriraman P, Bohini S, Schraeml M, Singh U, Brandt M et al. (2013) Target-mediated drug disposition and prolonged liver accumulation of a novel humanized anti-CD81 monoclonal antibody in cynomolgus monkeys. *MAbs* **5**:776–786.

Wen MS and Lee MT (2013) Warfarin Pharmacogenetics: New Life for an Old Drug. *Zhonghua Minguo Xinzangxue Hui Zazhi* **29**:235–242.

Wright DF and Duffull SB (2013) A Bayesian dose-individualization method for warfarin. *Clin Pharmacokinet* **52**:59–68.

Xue L, Holford N, Ding XL, Shen ZY, Huang CR, Zhang H, Zhang JJ, Guo ZN, Xie C, Zhou L et al. (2017) Theory-based pharmacokinetics and pharmacodynamics of S- and R-warfarin and effects on international normalized ratio: influence of body size, composition and genotype in cardiac surgery patients. *Br J Clin Pharmacol* **83**:823–835.

Yamazaki S, Shen Z, Jiang Y, Smith BJ, and Vicini P (2013) Application of target-mediated drug disposition model to small molecule heat shock protein 90 inhibitors. *Drug Metab Dispos* **41**:1285–1294.

Zheng S, Gaitonde P, Andrew MA, Gibbs MA, Lesko LJ, and Schmidt S (2014) Model-based assessment of dosing strategies in children for monoclonal antibodies exhibiting target-mediated drug disposition. *CPT Pharmacometrics Syst Pharmacol* **3**:e138.

Address correspondence to: Dr. Richard C. Brundage, University of Minnesota, 717 Delaware St. SE, Room 464, Minneapolis, MN 55455. E-mail: brund001@umn.edu